

## Catenation of Self-Assembled Nanorings

**Shiki Yagai,<sup>\*[a]</sup> Yusaku Goto,<sup>[a]</sup> Takashi Karatsu,<sup>[a]</sup> Akihide Kitamura,<sup>[a]</sup> and Yoshihiro Kikkawa<sup>[b]</sup>**

Construction of complex nanoscale architectures from small molecular building blocks (SMBBs) by programmed hierarchical organization processes is one of the most exciting frontiers of supramolecular chemistry and self-organization.<sup>[1]</sup> Understanding the complexity in the self-organization of biopolymers by using simplified artificial molecules in addition to discovering novel physicochemical functions in extended or discrete nanoarchitectures are major objectives in these studies. Among the various nanoarchitectures based on SMBBs,<sup>[2]</sup> toroidal or ring-shaped structures (nanorings) formed by end-to-end closing of fibrous supramolecular polymers (self-assembled nanofibers)<sup>[3]</sup> are new types of discrete nano-objects that have been reported by Lee et al. for amphiphilic molecules,<sup>[4]</sup> by the present authors for hydrogen bonded supermacrocycles (rosettes),<sup>[5]</sup> and by Parquette et al. for amphiphilic naphthalene diimides.<sup>[6]</sup> Although microscale circular architectures based on SMBBs have been previously reported, the formation mechanisms were explained by dewetting processes on the substrates.<sup>[7]</sup> In contrast, nanorings are believed to be already present in solution on the basis of dynamic light scattering (DLS) experiments, similar to the nanorings formed by amphiphilic block copolymers.<sup>[8]</sup> However, no direct evidence can be obtained by light scattering studies of solutions. In the present study, we report the formation of a topologically nontrivial nanostructure that can be regarded as visual evidence for the formation of nanorings in solution.

The nanorings under investigation are composed of  $\pi$ -electronic SMBBs, and are unique because they are formed hierarchically by hydrogen bonded supermacrocycles.<sup>[5]</sup> The formation of nanorings is believed to be caused by the specific curvature encoded within the  $\pi$ - $\pi$  stacked columnar nanostructures of the supermacrocycles formed in nonpolar

solvents under dilute conditions. The system that meets the three requirements for further advance of this nanoring research, that is: 1) simple molecular design, 2) uniformly sized nanorings, and 3) mechanical stiffness against atomic force microscopy (AFM) imaging, is evolved from the oligo(*p*-phenylenevinylene) **1**, which is asymmetrically substituted with a barbituric acid (BAR) hydrogen bonding group and a wedge-shaped<sup>[1c]</sup> aliphatic tail (Figure 1a).<sup>[5b]</sup> This “BAR- $\pi$ -wedge” molecule<sup>[9]</sup> forms nanorings with di-

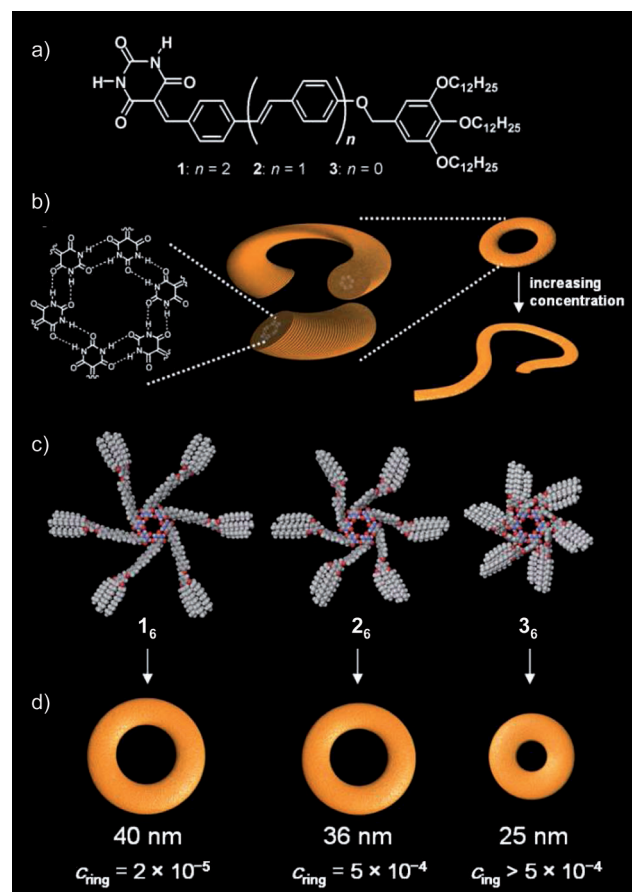


Figure 1. a) Chemical structures of **1–3**. b) Proposed mechanism for the formation of nanorings and nanofibers by hydrogen bonded supermacrocycles. Other hydrogen bonding patterns can also produce supermacrocycles, see Figure S1 in the Supporting Information. c) Molecular modeled hexameric supermacrocycles of **1–3**. d) Comparison of nanoring size (estimated by AFM) formed by **1–3** with typical edge-to-edge widths and concentration threshold for their predominant formation ( $c_{\text{ring}}$ ).

[a] Prof. Dr. S. Yagai, Y. Goto, Prof. Dr. T. Karatsu, Prof. Dr. A. Kitamura  
Department of Applied Chemistry and Biotechnology  
Graduate School of Engineering, Chiba University  
1-33 Yayoi-cho, Inage-ku, Chiba 263-8522 (Japan)  
Fax: (+81) 43-290-3039  
E-mail: yagai@faculty.chiba-u.jp

[b] Dr. Y. Kikkawa  
Photonics Research Institute  
National Institute of Advanced Industrial Science and Technology  
1-1-1 Higashi, Tsukuba, Ibaraki 305-8562 (Japan)

Supporting information for this article is available on the WWW under <http://dx.doi.org/10.1002/chem.201102982>.

ameters of about 40 nm when dissolved in methylcyclohexane (MCH). However, the nanorings are predominantly formed only at very low concentrations of less than  $4 \times 10^{-5}$  M, and upon increasing concentration, a transition to open-ended nanofibers and to stiff nanorods resulted (Figure 1 b). We herein report that the attempt to refine the molecular structure toward the exclusive formation of nanorings leads to compounds **2** and **3**, which predominantly afford nanorings in a significantly higher concentration regime compared to **1**, due to weakened  $\pi$ - $\pi$  stacking interactions (thus, a reduction in the degree of supramolecular polymerization of the supermacrocycles). Furthermore, nanorings formed by **2** are of similar size to those of **1**, and they are formed in solution at higher concentrations, and thus allow the interlocking (catenation) of two self-assembled nanorings. The formation of *self-assembled catenane* is prima facie evidence for the formation of these nanorings in solution.

Compounds **2** and **3** formed thermotropic liquid crystals between 144–162 and 109–138 °C, respectively, which exhibited birefringent textures characteristic of the columnar organization of discotic entities.<sup>[10]</sup> These mesophases had X-ray diffraction peaks that were assignable to rectangular columnar ( $\text{Col}_r$ ) ordering with lattice parameters  $a/b = 6.7/6.1$  nm for **2** and 5.8/5.1 nm for **3** (Figure 2 a). The formation of  $\text{Col}_r$  structures with relatively large lattice parameters compared to their extended molecular lengths (**2**: 3.7 nm, **3**: 3.1 nm) demonstrates the columnar organization of these molecules through the formation of hydrogen bonded supermacrocycles (Figure 1 b).<sup>[11]</sup> Furthermore, the rectangular ordering of the columns is indicative of slipped stacks of the supermacrocycles,<sup>[11c–e]</sup> which is similar to that observed for **1**.<sup>[5b]</sup>

Both the  $\text{Col}_r$  structures of **2** and **3** did not exhibit intracolumnar periodicity corresponding to the lattice parameter  $c$  (center-to-center distance of the supermacrocycles). Therefore, we calculated the number of molecules per unit slice of a column ( $Z$  value)<sup>[12]</sup> by varying

$c$  values from 3.5 to 6 Å and assuming a density of 1.0 g cm<sup>-3</sup>.<sup>[13]</sup> For **2**, the  $Z$  value changed from 4.4 to 7.6, and for **3**, it changed from 3.5 to 6.0 (Figure 2 b). For **1** with lattice parameters  $a/b = 8.3/7.5$  nm,<sup>[5b]</sup>  $Z$  varied from 6.1 to 10. All the compounds most likely form supermacrocycles based on the same hydrogen bonded motif (i.e., the same  $Z$  values); therefore, the analysis illustrates that the reduction of  $\pi$  segments (**1**→**2**→**3**) results in augmentation of the  $c$  values (3.4→4.8→6.0 Å when  $Z$  is fixed to 6). This result is reasonable because the peripheral wedges in the supermacrocycles become crowded upon reducing the  $\pi$  segments (Figure 1 c); this enlarges the slipping and/or the interdisc distance within columns (Figure 2 c). Such a modulatable stacking fashion of the supermacrocycles by the alteration

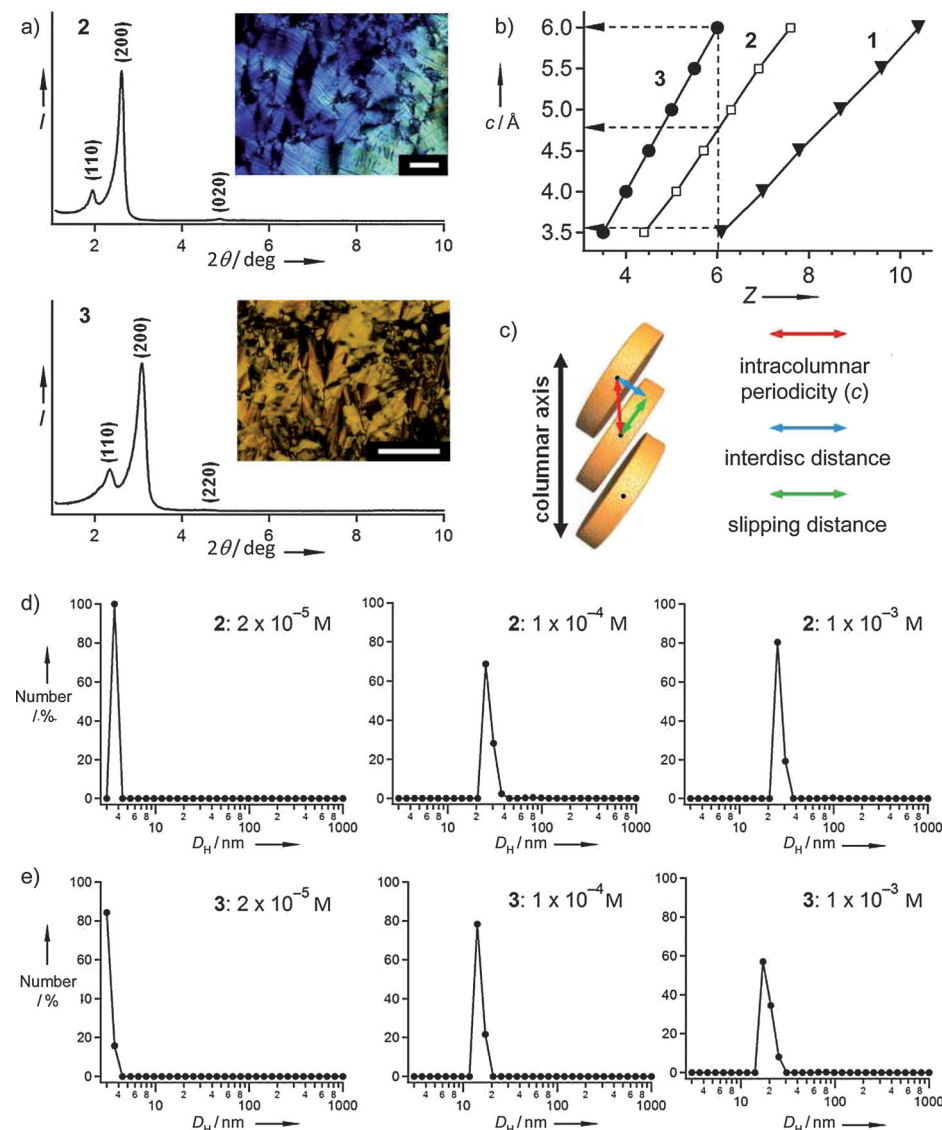


Figure 2. a) X-ray diffraction patterns of **2** at 150 °C (top) and **3** at 130 °C (bottom). Insets: polarized optical micrographs (scale bar: 50 µm). b) Plot of calculated number of molecules per unit slice of column ( $Z$  value) versus intracolumnar periodicity  $c$  (3.5–6.0 Å) for the  $\text{Col}_r$  structures of **1**–**3**. c) Schematic representation of stacked discotic supermacrocycles. Hydrodynamic diameter ( $D_H$ ) distributions measured by DLS of MCH solutions of: d) **2**, and e) **3** at three different concentrations of (from left to right)  $2 \times 10^{-5}$ ,  $1 \times 10^{-4}$  and  $1 \times 10^{-3}$  M.

of the  $\pi$  conjugation length has a significant impact on the solution phase organization, as described below.

Nanostructures of **2** and **3** were prepared by dissolving small amounts of the compounds in MCH with heating, and then cooling the resulting homogeneous solution to room temperature. Temperature-dependent UV/Vis spectroscopy showed the growth of red-shifted absorption bands upon cooling from 90 to 20°C (Figure S2 in the Supporting Information); this indicates the formation of  $\pi$ - $\pi$  stacked aggregates. DLS measurements of  $2 \times 10^{-5}$  M solutions indicated only small aggregates (or monomers) with hydrodynamic diameters ( $D_H$ ) less than 4 nm (Figure 2d and e). Upon increasing the concentrations above  $1 \times 10^{-4}$  M, both compounds showed the formation of nanostructures with average  $D_H$  of 30 nm for **2** and 20 nm for **3**. Interestingly, the  $D_H$  of these compounds did not change when the concentrations were increased to  $1 \times 10^{-3}$  M. These results are in sharp contrast to that of **1**, which displayed a significant increase of  $D_H$  when the concentration was increased from  $2 \times 10^{-5}$  M (ca. 60 nm, nanoring) to  $1 \times 10^{-4}$  M (ca. 300 nm, open-ended nanostructures).

The nanostructures formed by **2** and **3** in MCH were spin-coated onto highly oriented pyrolytic graphite (HOPG) and imaged by using AFM. Although the specimens prepared by drop-casting displayed nanostructures identical to those prepared by spin-coating, we avoided the former preparation method to prevent unfavorable agglomeration of nanostructures. The specimens prepared from a  $1 \times 10^{-4}$  M solution of **2** displayed a large number of nanorings with high uniformity of size and shape (Figure 3a and Figure S3 in the Supporting Information). Open-ended structures, such as curved fibrils, spirals and stiff rods, which were all observed for **1** at the same concentration, were rarely found in repeated imaging of the specimens. The typical width of nanorings (edge-to-edge distance) was 36 nm, which is slightly shorter than that for **1** by 4 nm (Figure 1d).

A considerable amount of nanorings (ca. 60% of all nanostructures) was imaged even for specimens prepared from  $5 \times 10^{-4}$  M solution of **2** (Figure 3b). This situation is comparable to the specimen prepared from a  $4 \times 10^{-5}$  M solution of **1**. Closer inspection of the AFM images revealed the presence of interlocked structures of two nanorings (circled areas in Figure 3b).<sup>[14]</sup> Figure 3c–e show magnified images of the catenated nanostructures. One of the two contact parts of the interlocked nanorings, for example, the contact point *x* of rings A and B in Figure 3d, has identical height to the main body of nanorings (ca. 1.8 nm). At such a point, the upper-lying nanoring is clearly discernible from the AFM image (i.e., ring A). Another contact point, that is, point *y*, exhibits a higher height (2.6 nm) than the main body of nanorings. For such a point, cross-sectional analyses along to ring A (Figure 3f) and B (Figure 3g) gave different height profiles, and revealed that ring B is the upper-lying nanostructure at this contact point. It can be concluded from these analyses that the two nanorings are interlocked with each other and not simply overlapped nanostructures. Approximately one or two catenanes were found in every

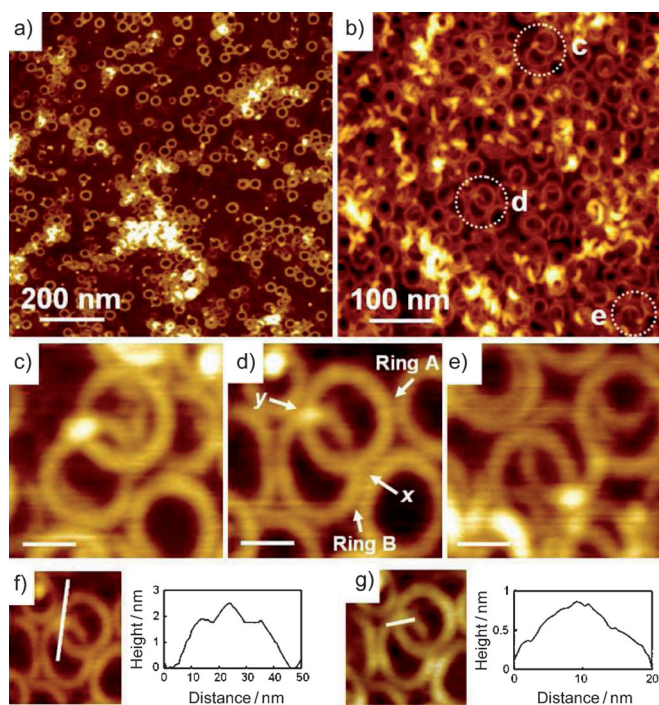


Figure 3. AFM height images of nanostructures of **2** spin-coated (3000 rpm) from MCH solutions at concentrations of: a)  $1 \times 10^{-4}$ , and b)  $5 \times 10^{-4}$  M onto HOPG (z scale: 20 nm). c)–e) Magnified images of the catenated nanorings found in the circled areas in (b); scale bar: 20 nm. f), g) Cross-sectional analysis of the catenane in (d).

$200 \times 200$  nm area (Figure S4 in the Supporting Information). Because single nanorings are composed of approximately 1300 molecules of **2**,<sup>[15]</sup> this finding indicates an unprecedented type of supramolecular catenanes that consists of more than 2000 molecules of the SMBBs.

Further reduction of the  $\pi$  segments in the present “BAR- $\pi$ -wedge” system resulted in the almost exclusive formation of nanorings. Thus, specimens of **3** exhibited a number of nanorings, despite being prepared from  $5 \times 10^{-4}$  M solutions (Figure 4a). Although other open-ended structures are rarely found, the presence of small spherical nanostructures should be noted. Such nanostructures can be produced

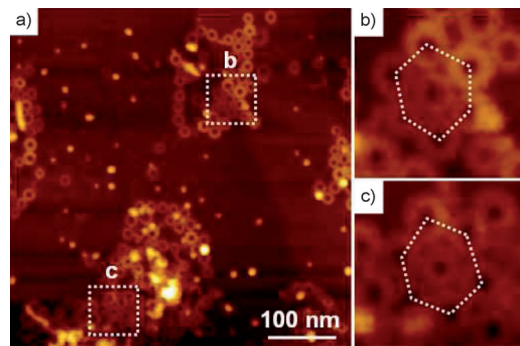


Figure 4. a) AFM height image of a sample prepared by spin-coating of a MCH solution of **3** ( $5 \times 10^{-4}$  M) onto HOPG (z scale: 20 nm). b), c) Magnified images of the square areas indicated in (a).

through the nonspecific aggregation of monomeric **3** (or its hydrogen bonded supermacrocycles) upon evaporation of the solvent. Another notable feature of the nanorings of **3** is that they tend to be closely arranged on the surface and exhibit pseudohexagonal packing motifs (Figure 4b and c). This is different from that of **1** and **2** and could be related to the degree of shape-persistence of the toroidal nanostructures. The typical size of the nanorings of **3** is 25 nm, which is significantly smaller than that of **2** (Figure 1d). The size reduction could render stiffer nanorings, which would enable their two-dimensional organization. As a result of the size reduction, catenation was not observed for **3**.

Catenane, an interlocked structure of two or more macrocyclic molecules, has attracted the attention of chemists not only for topological curiosity, but also from a functional viewpoint.<sup>[14,16]</sup> Catenation of macromolecular entities, such as DNA, has long been known<sup>[17]</sup> and has been analyzed by AFM.<sup>[18]</sup> Recently, Deffieux et al. have succeeded in visualizing catenation of grafted polymers by using AFM.<sup>[19]</sup> To our knowledge, the present study is the first time catenation of purely self-assembled nanofibers has been visualized by AFM. Arguably, the formation of self-assembled catenanes composed of SMBBs requires the occurrence of a large number of well-defined toroidal aggregates in solution upon cooling for statistical reasons. Such requirements are fulfilled in the present study by the reduction of  $\pi$  segments in “BAR- $\pi$ -wedge” designed molecules. The supramolecular organization of “BAR- $\pi$ -wedge” molecules could, therefore, provide further unique nanostructures by minor structural modulation that could exhibit interesting nanoscopic functionality.

**Keywords:** catenane • hydrogen bonds • nanostructures • self-assembly • supramolecular chemistry

- [1] a) G. M. Whitesides, B. Grzybowski, *Science* **2002**, *295*, 2418–2421; b) J.-M. Lehn, *Science* **2002**, *295*, 2400–2403; c) B. M. Rosen, C. J. Wilson, D. A. Wilson, M. Peterca, M. R. Imam, V. Percec, *Chem. Rev.* **2009**, *109*, 6275–6540.
- [2] A. C. Grimsdale, K. Müllen, *Angew. Chem.* **2005**, *117*, 5732–5772; *Angew. Chem. Int. Ed.* **2005**, *44*, 5592–5629.
- [3] L. Brunsved, B. J. Folmer, E. W. Meijer, R. P. Sijbesma, *Chem. Rev.* **2001**, *101*, 4071–4098.
- [4] a) J.-K. Kim, E. Lee, Z. Huang, M. Lee, *J. Am. Chem. Soc.* **2006**, *128*, 14022–14023; b) E. Lee, Y.-H. Jeong, J.-K. Kim, M. Lee, *Macromolecules* **2007**, *40*, 8355–8360; c) E. Lee, J.-K. Kim, M. Lee, *J. Am. Chem. Soc.* **2009**, *131*, 18242–18243; d) I.-S. Park, Y.-R. Yoon, M. Jung, K. Kim, S. Park, S. Shin, Y.-b. Lim, M. Lee, *Chem. Asian J.* **2011**, *6*, 452–458.
- [5] a) S. Yagai, S. Mahesh, Y. Kikkawa, K. Unoike, T. Karatsu, A. Kitamura, A. Ajayaghosh, *Angew. Chem.* **2008**, *120*, 4769–4772; *Angew. Chem. Int. Ed.* **2008**, *47*, 4691–4694; b) S. Yagai, S. Kubota, H. Saito, K. Unoike, T. Karatsu, A. Kitamura, A. Ajayaghosh, M. Kanesato, Y. Kikkawa, *J. Am. Chem. Soc.* **2009**, *131*, 5408–5410; c) S. Yagai, H. Aonuma, Y. Kikkawa, S. Kubota, T. Karatsu, A. Kitamura, S. Mahesh, A. Ajayaghosh, *Chem. Eur. J.* **2010**, *16*, 8652–8661.
- [6] H. Shao, J. Seifert, N. C. Romano, M. Gao, J. J. Helmus, C. P. Jaroenie, D. A. Modarelli, J. R. Parquette, *Angew. Chem.* **2010**, *122*, 7854–7857; *Angew. Chem. Int. Ed.* **2010**, *49*, 7688–7691.
- [7] a) A. P. H. J. Schenning, F. B. G. Benneker, H. P. M. Geurts, X. Y. Liu, R. J. M. Nolte, *J. Am. Chem. Soc.* **1996**, *118*, 8549–8552; b) H. A. M. Biemans, A. E. Rowan, A. Verhoeven, P. Vanoppen, L. Latterini, J. Foekema, A. P. H. J. Schenning, E. W. Meijer, F. C. De Schryver, R. J. M. Nolte, *J. Am. Chem. Soc.* **1998**, *120*, 11054–11060; c) T. Vossmeyer, S.-W. Chung, W. M. Gelbart, J. R. Heath, *Adv. Mater.* **1998**, *10*, 351–353; d) S. Masuo, H. Yoshikawa, T. Asahi, H. Masuhara, T. Sato, D.-L. Jiang, T. Aida, *J. Phys. Chem. B* **2001**, *105*, 2885–2889; e) M. C. Lenssen, K. Takazawa, J. A. A. W. Elemans, C. R. L. P. N. Jeukens, P. C. M. Christianen, J. C. Maan, A. E. Rowan, R. J. M. Nolte, *Chem. Eur. J.* **2004**, *10*, 831–839; f) O. J. Dautel, M. Robitzer, J.-C. Flores, D. Tondelier, F. Serein-Spirau, J.-P. Lère-Porte, D. Guérin, S. Lenfant, M. Tillard, D. Vuillaume, J. J. E. Moreau, *Chem. Eur. J.* **2008**, *14*, 4201–4213.
- [8] a) D. J. Pochan, Z. Chen, H. Cui, K. Hales, K. Qi, K. L. Wooley, *Science* **2004**, *306*, 94–97; b) H. Huang, B. Chung, J. Jung, H.-W. Park, T. Chang, *Angew. Chem.* **2009**, *121*, 4664–4667; *Angew. Chem. Int. Ed.* **2009**, *48*, 4594–4597.
- [9] For other barbiturate-functionalized molecules forming different nanoarchitectures, see: a) X. Huang, C. Li, S. Jiang, X. Wang, B. Zhang, M. Liu, *J. Am. Chem. Soc.* **2004**, *126*, 1322–1323; b) S. Yagai, T. Kinoshita, Y. Kikkawa, T. Karatsu, A. Kitamura, Y. Honsho, S. Seki, *Chem. Eur. J.* **2009**, *15*, 9320–9324; c) S. Yagai, Y. Nakano, S. Seki, A. Asano, T. Okubo, T. Isoshima, T. Karatsu, A. Kitamura, Y. Kikkawa, *Angew. Chem.* **2010**, *122*, 10186–10190; *Angew. Chem. Int. Ed.* **2010**, *49*, 9990–9994; d) C.-C. Chu, G. Raffy, D. Ray, A. D. Guerzo, B. Kauffmann, G. Wantz, L. Hirsch, D. M. Bassani, *J. Am. Chem. Soc.* **2010**, *132*, 12717–12723.
- [10] For the synthesis and characterization, see the Supporting Information.
- [11] a) T. Kato, N. Mizoshita, K. Kishimoto, *Angew. Chem.* **2005**, *118*, 44–74; *Angew. Chem. Int. Ed.* **2005**, *45*, 38–68; b) H. M. Keizer, R. P. Sijbesma, *Chem. Soc. Rev.* **2005**, *34*, 226–234; c) S. Jin, Y. Ma, S. C. Zimmerman, S. Z. D. Cheng, *Chem. Mater.* **2004**, *16*, 2975–2977; d) S. Yagai, T. Nakajima, K. Kishikawa, S. Kohmoto, T. Karatsu, A. Kitamura, *J. Am. Chem. Soc.* **2005**, *127*, 11134–11139; e) F. Vera, R. M. Tejedor, P. Romero, J. Barberá, M. B. Ros, J. L. Serrano, T. Sierra, *Angew. Chem.* **2007**, *119*, 1905–1909; *Angew. Chem. Int. Ed.* **2007**, *46*, 1873–1877.
- [12] a) S. Yagai, S. Kubota, T. Iwashima, K. Kishikawa, T. Nakanishi, T. Karatsu, A. Kitamura, *Chem. Eur. J.* **2008**, *14*, 5246–5257.
- [13] G. Ungar, V. Percec, M. N. Holerca, G. Johansson, J. A. Heck, *Chem. Eur. J.* **2000**, *6*, 1258–1266.
- [14] *Synthetic DNA Topology, Molecular Catenanes, Rotaxanes and Knots* (Eds.: J.-P. Sauvage, D. Dietrich-Buchecker), Wiley-VCH, Weinheim, 1999.
- [15] For the calculation, see the Supporting Information.
- [16] N. C. Seeman in *Synthetic DNA Topology, Molecular Catenanes, Rotaxanes and Knots* (Eds.: J.-P. Sauvage, D. Dietrich-Buchecker), Wiley-VCH, Weinheim, 1999, pp. 323–356.
- [17] a) B. Champin, P. Mobian, J.-P. Sauvage, *Chem. Soc. Rev.* **2007**, *36*, 358–366; b) E. R. Kay, D. A. Leigh, F. Zerbetto, *Angew. Chem.* **2007**, *119*, 72–196; *Angew. Chem. Int. Ed.* **2007**, *46*, 72–191; c) M. D. Lankshear, P. D. Beer, *Acc. Chem. Res.* **2007**, *40*, 657–668.
- [18] H. Yamaguchi, K. Kubota, A. Harada, *Nucleic Acids Symp. Ser.* **2000**, 229–230.
- [19] M. Schappacher, A. Deffieux, *Angew. Chem.* **2009**, *121*, 6044–6047; *Angew. Chem. Int. Ed.* **2009**, *48*, 5930–5933.

Received: September 22, 2011  
Published online: November 3, 2011